Probing the analytic Cancellation Factor relationship using mesospheric nightglows and lidar observations obtained at the Andes Lidar Observatory

Javier Fuentes[1,2], Fabio Vargas[3]
[1] Department of Physics, University of La Serena, La Serena, Chile.
[2] Gemini Observatory, La Serena, Chile.
[3] Department of Electrical and Computer Engineer, University of Illinois, Urbana, Illinois, USA.

Introduction

We present the first study to test the theoretical relationship of the Cancellation Factor (CF) using T/W Na Lidar data and zenith night airglow observations of the OH and O(^{1}S) emissions. The dataset analyzed was obtained during the observing campaigns in 2015, 2016, and 2017 at the Andes Lidar Observatory (ALO) in Chile. We have used two empirical methods to fit the analytical function described in [1] upon the assumption of having saturated waves (damping factor, $\beta = 1$), vertically propagating waves, and windless atmosphere.

We report that the analytical relationship underestimates the observational model after correcting the models using the weighted mean as described in [2]. We obtained a good agreement respect to the theoretical value for O(^{1}S) emission line. In contrast, the observational model deviate by a factor of ~2 from the theoretical value for the OH Meinel emission band. The disagreement might mainly come from the fact that dissipative and freely propagating waves co-exist with saturated waves, and we have not separated waves by their kind in this study.

These important measurements provide a useful information to identify the waves as coherent wave events deduced from zenith and off-zenith observations of the layers using combined spatial (2-D) and temporal (1-D) imaging and lidar data with the aim to understand the fundamental mechanisms that causes the variation of the phase and amplitude of the airglow in response to the Atmospheric Gravity Waves (AGWs) for multiple layers through the MLT region.

Data

The dataset analyzed was obtained during the observing campaigns in 2015, 2016, and 2017 at the Andes Lidar Observatory (ALO) in Chile. We used T/W Na Lidar data and zenith night airglow observations of the OH and O(^{1}S) emissions.

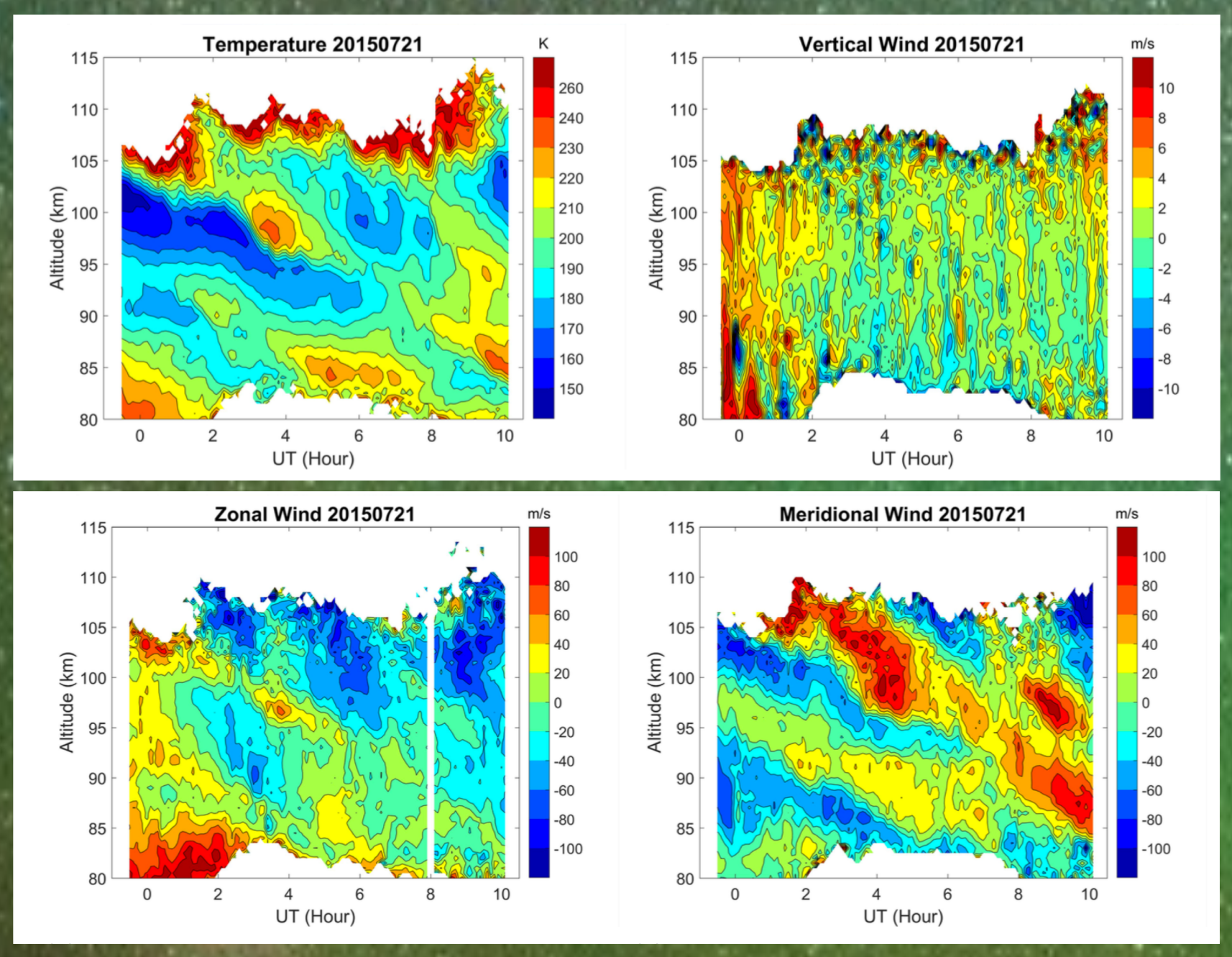

Figure 1. Temperature and winds Na lidar profiles.

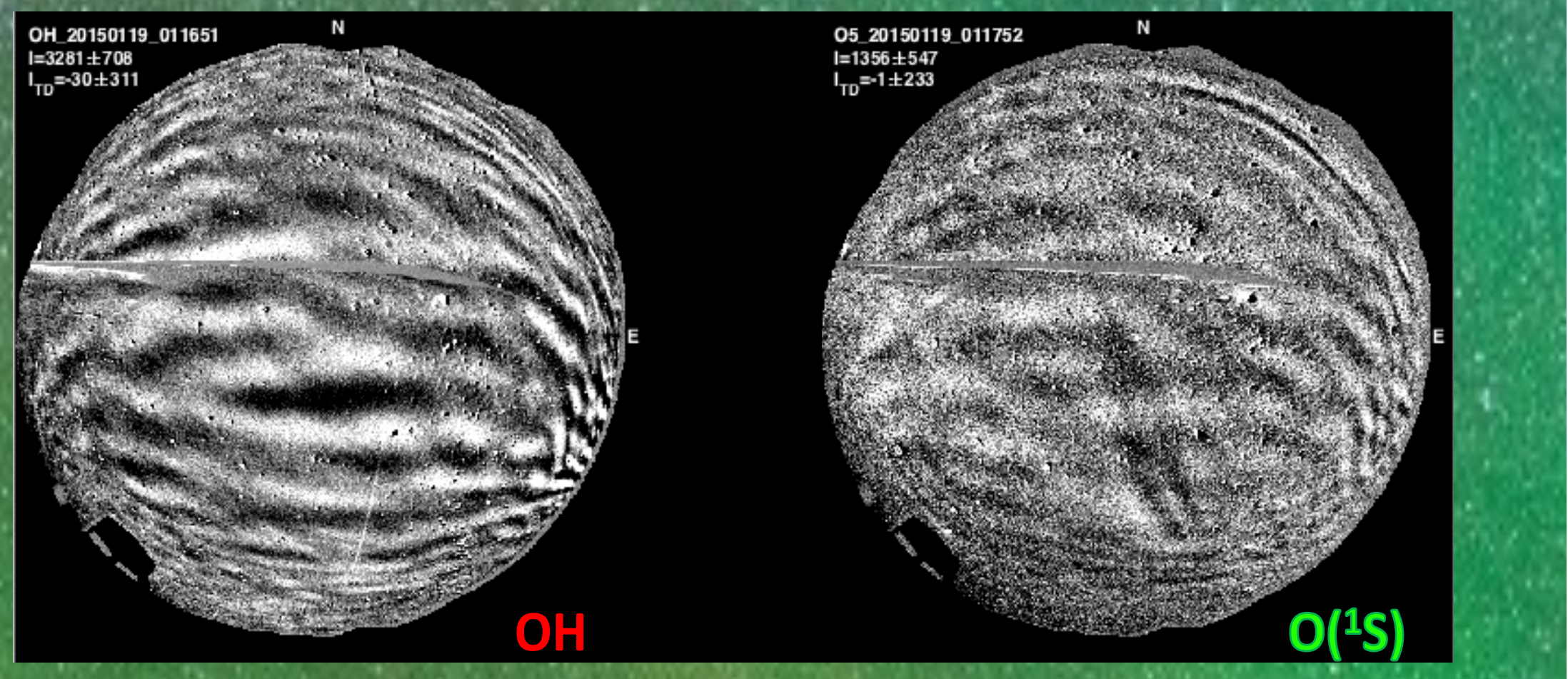

Figure 2. OH and O(^{1}S) night airglow emissions captured through the All-Sky-Imager at ALO.

The Na lidar was operated in zenith mode and off-zenith modes. The integration time in each direction varies between campaigns from 60 to 90 sec which depends on the signal retrieved.

The filter set used and exposure times for the All-Sky-Imager are as seen in the table 1:

Filter	λ_{center} (nm)	FWHM (nm)	Exp. time (sec)
O(^{1}S) BG	551.0	3	60
O(^{1}S)	557.7	3	90
O(^{1}D)	630.0	3	75
OH(6-2)	840.0	20	60
O_2(0-1)	866.0	7	45

Table 1. The O(^{1}S) and OH(6-2) filters were used to estimate the wave amplitude based on the analytical model relating volume emission rate measured by the night airglow images to the relative atmospheric density perturbation described by [2].

Site

The Andes Lidar Observatory (ALO) is located at 30.3S, 70.7W at an altitude of 2530 m on top of Cerro Pachon mountain, Chile.

Figure 3. Panoramic view of the center of operations which hosts passive instrumentation managed to the efforts of the Remote Sensing and Space Laboratory (RSSS) of the University of Illinois at Urbana-Champaign (UIUC) and the Embry-Riddle Aeronautical University at Florida, United States.

Instrumentation

The instrumentation used were a Na resonance-fluorescence lidar which measures temperature, wind velocity, and Na density profiles typically at resolution of 1 min, 500 m between 80 – 105 km; and an All-Sky-Imager records airglow images of hydroxyl (OH) and atomic oxygen line emissions. ALO is equipped with a suite of passive optical instruments and a new meteor radar being built next to the center of operations.

Figure 4. The a) and b) photographs were taken outside the center of operations at the Andes Lidar Observatory (ALO) in Chile. In both images of long exposures can be seen the propagation directions of the Na lidar observations, whereas only in b) can be observed the airglow layers at lower elevations over the Andes Mountain range and the stars trails projected over the Southern sky. In c) is shown the optical bench of the Sodium laser. Finally, the picture in d) shows the All-Sky-Imager (ASI 1 & 2) including the detail of the CCD type and filter wheel setup displayed in the inset.

Methodology

In this study we report perturbations in the airglow intensity in response to the Atmospheric Gravity Waves (AGWs) through the wave cancellation effect using two methods:

Direct Method: The Cancellation Factor (CF) is measured by the ratio of the amplitude of I' or T' to the amplitude of the perturbing AGW at 88 km for OH Meinel band emission and 95 km for O(^{1}S) emission line. The CF can thus be defined for the airglow intensity as $\mathrm{CF_I} = \mathrm{A}_I/\mathrm{A}_T$. Here, $\mathrm{A}_I = I'/\bar{I}$ and $\mathrm{A}_T = T'/\bar{T}$, where primed quantities refer to the wave fluctuation and bar quantities to the unperturbed background. Here, A_I is obtained from image processing and A_T from the lidar temperature data at the time of wave perturbation.

FFT Method: The CF is derived using the same definition than method 1, but the temperature wave fluctuation (T') term in the A_T ratio is computed from the Discrete Fourier Transform using the lidar temperature data at the time of wave perturbation event.

Results

- The Cancellation Factor (CF) increases monotonically with λ_z < 13.9 km for OH band emission and λ_z < 10.4 km for O(^{1}S) emission line, therefore, for λ_z lower than these limits the cancellation effect become stronger.
- The uncertainties estimated in σ_{λ_z} for both methods in the OH band and O(^{1}S) emission are ~16% and ~17% which are in a good agreement to the uncertainties reported in [2]. The uncertainties in σ_{CF} for the OH and O(^{1}S) emissions were estimated in ~10% and ~7% for both methods.

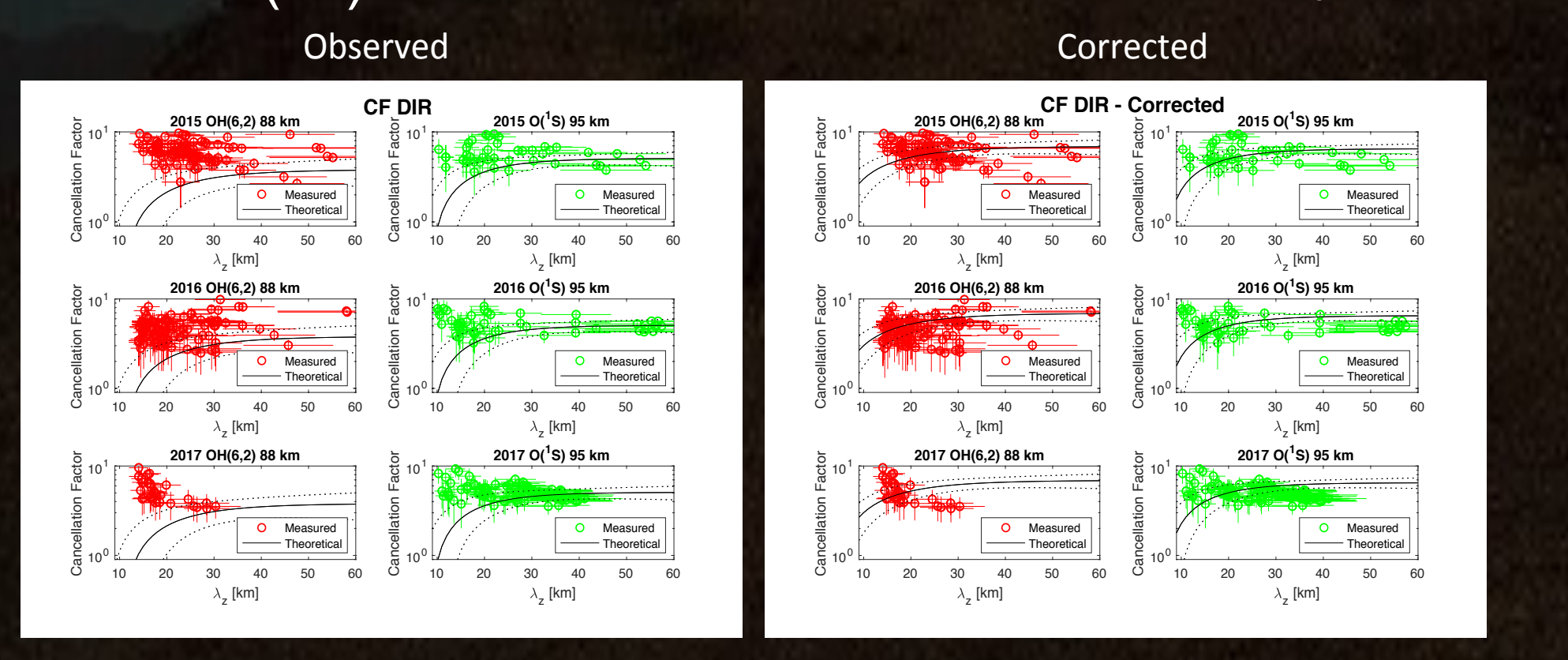

Figure 5. The Cancellation Factor for the direct method.

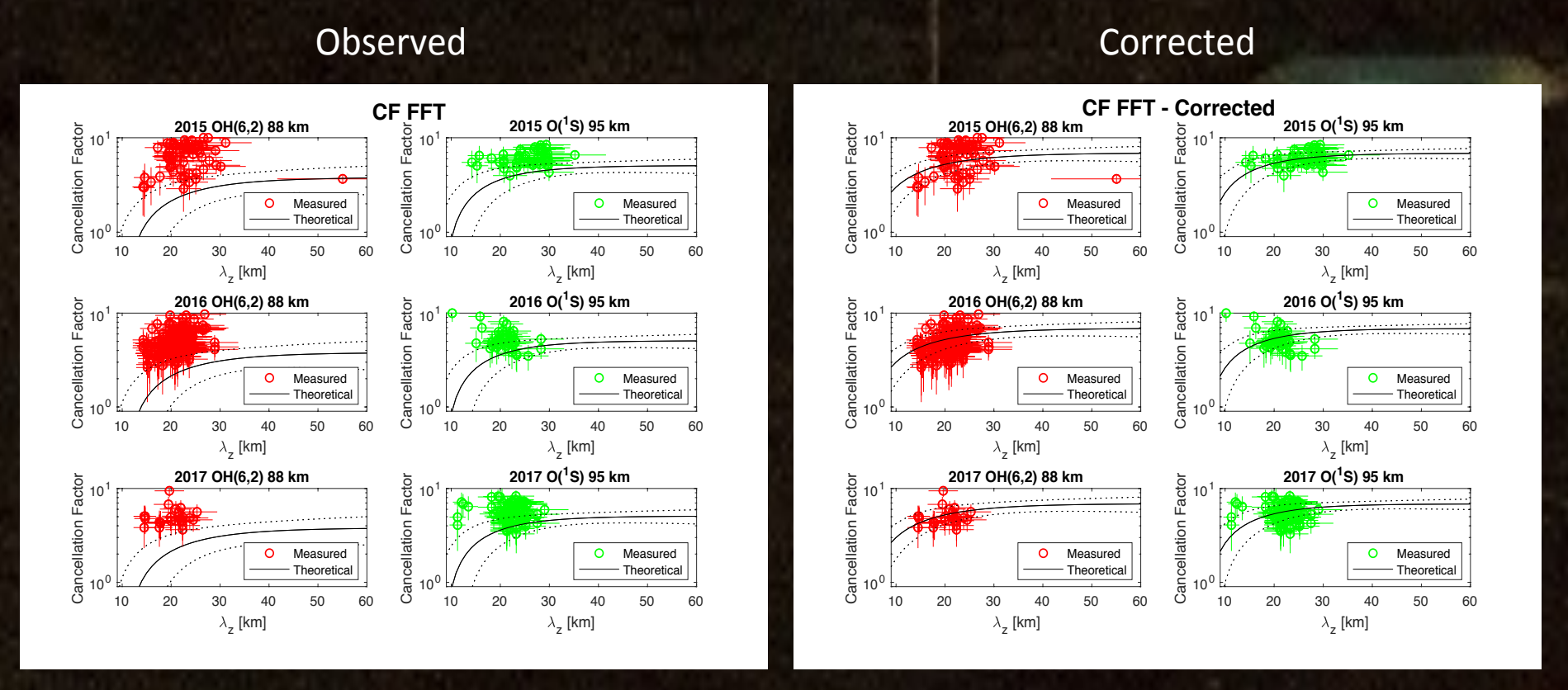

Figure 6. The Cancellation Factor for the FFT method.

- The Fig. 5 and Fig. 6 show the CF for both OH (red open circles) and O(^{1}S) (green open circles) emissions and their errors. The dashed thin lines denotes the 95% confidence bounds around the theoretical curve showed as the continuous black lines.
- After correcting the CF by the weighted mean and weighted errors computed for the direct method we obtained a good agreement to the theoretical value, $\mathrm{CF_{theo}} = 5.1$, for the O(^{1}S) emission line in 2015, 2016, and 2017. In contrast, we did not find a good correlation for the OH emission as the estimated weighted mean is higher to the theoretical value, $\mathrm{CF_{theo}} = 3.8$, by a factor of ~2.
- We did not find a good correlation for the FFT method at any of both emission lines after correcting the CF by the weighted mean and their errors.

References

[1] Vargas, F. A., Swenson, G., Liu, A., and Gobbi, D. (2007)
O(^{1}S), OH, and O_2(b) airglow layer perturbations due to AGWs and their implied effects on the atmosphere.
J. Geophys. Res., 112, D14102, DOI:10.1029/2006JD007642.
[2] Vargas, F. A (2018)
Uncertainties in Momentum Flux and Accelerations due to Gravity wave Parameters Estimated from Mesospheric Nightglows.
DOI: 10.1016/j.asr.2018.09.039

CEDAR workshop
June 16-21, 2019
Santa Fe, NM.
www.cedarweb.vsp.ucar.edu/